Journal of KONBiN 2022
Volume 52, Issue 1
DOI 10.2478/jok-2022-0010

AGNIESZKA KOSOŃ-SCHAB
AGH University of Science and Technology (Akademia Górniczo-Hutnicza)

INFLUENCE OF THE CRANE LOAD AND MEASUREMENT SPEED ON THE PROPERTIES OF THE MAGNETIC FIELD OF THE GIRDERS
Wpływ obciążenia suwnicy i prędkości pomiarowej na własności pola magnetycznego dźwigarów

Abstract: *The girders of the crane or the jib of the crane are situated at high heights, which prevents the free and continuous measurement of their stresses. Unfortunately, these elements are most exposed to high stress and damage during their use. The article presents the research methodology with the use of the magnetic metal memory method of the overhead crane girders. Diagnostic tests utilizing the crane movement mechanisms to move the magnetometric sensor along the tested surface of the girder were proposed to improve and automate measurements. The article attempts to investigate effect of the device load and speed of Hp measurements with a magnetometric sensor.*
Keywords: metal magnetic memory, magnetic field non-destructive evaluation, diagnostics, overhead crane.

Streszczenie: *Dźwigary suwnicy usytuowane są na dużych wysokościach, co uniemożliwia swobodny i ciągły pomiar ich naprężeń. Niestety elementy te są najbardziej narażone na duże obciążenia i uszkodzenia podczas ich użytkowania. W artykule przedstawiono metodykę badań z wykorzystaniem metody magnetycznej pamięci metalowej dźwigarów suwnic. Zaproponowano badania diagnostyczne wykorzystujące mechanizmy ruchu suwnic (wózek wciągarki) do przemieszczania czujnika magnetometrycznego po badanej powierzchni dźwigara w celu usprawnienia i zautomatyzowania pomiarów. W artykule podjęto próbę zbadania wpływu obciążenia urządzenia i prędkości pomiarów Hp za pomocą czujnika magnetometrycznego.*
Słowa kluczowe: magnetyczna pamięć metalu, natężenie pola magnetycznego, diagnostyka, suwnica.

1. Introduction

Lifting devices work under high and immediate load, thanks to this, it is possible to carry heavy loads. The structure of these devices is exposed to damage due to material fatigue. To ensure their correct and safe use, they should undergo continuous diagnostic tests.

The method of magnetic metal memory (MMM) has been developing for over 20 years. In practice, it is considered an effective NDT method for early detection of damage and determination of potential damage sites in ferromagnetic materials. It is based on the analysis of the distribution of the intrinsic self-magnetic leakage (SMFL) field on the surface of the product to identify (reveal) stress concentration zones (SCZ), defects, and inhomogeneities in the structure of the ferromagnetic material. The intrinsic scattering field intensity Hp [A/m] is the numerical value of the tangent and normal components of the magnetic scattering field, measured on the element's surface [3, 14].

The basics of the MMM method include the effect of magnetomechanical coupling of ferromagnetic materials, the basic characteristics of MMM signals induced by the concentration of stresses and defects are related to a weak magnetic field and external forces. The essence of the MMM method is the measurement and interpretation of the local magnetic field disturbance caused by local stresses in the material, local plastic deformation of the material, or the presence of material discontinuities, both mechanical (cracks, delamination) and structural (inclusions of other material). The measured values are the tangential and normal components of the magnetic field intensity H, measured near the diagnosed object [19].

$$H = \frac{B}{\mu_0 * \mu_r} \tag{1}$$

where:
B is the vertical value of the magnetic induction component *[T]*,
μ_0 is vacuum magnetic permeability *[4*π*10^{-7} H/m]*,
μ_r is relative vacuum magnetic permeability [-].

In the area of material inhomogeneity, the flux of the magnetic field intensity vector is disturbed and the flux leaks outside the tested element. If there is a defect in the tested material, the magnetometer shows a sharp change in the sign of the magnetic field intensity component resulting from the leakage of the vector flux of the magnetic field intensity. To learn more about the mechanisms of changing the magnetic field, tests were carried out on samples appropriately selected in terms of material quality, damage, and shape. The basic characteristics of the magnetic field strength signal were determined for the most common damage to the tested material samples [2, 15, 17]. Figure 1 shows the basic morphology of MMM signals developed based on the available literature by Shi P., Su S., Chen Z.

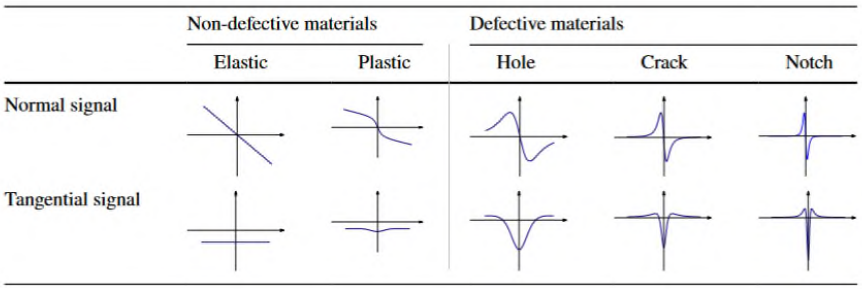

Fig. 1. The basic morphology of MMM signals [17]

The MMM signal near a defect or stress concentration has nonlinear characteristics. The tangent component Hx reaches its maximum value near the stress concentration or damage zone, then the normal Hy component is usually equal to 0. On this basis, we determine the location of the stress concentration or the damage zone identifying them using the position of the maximum value of the tangent component Hx and the zero characteristics of the normal component Hy.

The interval between the peak values of the normal component Hy and the peak value of the tangential component Hx is the effect of the size of the defect or the stress concentration. This knowledge allows us to say that the measurement of the signal characteristics can theoretically determine the size of the damage [7, 11]. It has been proved that the stresses resulting from tensile, compressive, and bending loads, acting over a long period, cause stress concentration in the loaded element. The verification tests were carried out on pipelines using the metal magnetic memory method. The stress concentration zones shown were compared with other methods of non-destructive testing to ensure the reliability of the method [3, 4, 20].

The changes of the magnetic distribution depending on the type of treatment and forming were also investigated [13]. The magnetic field strength level in a ferromagnetic material depends on its initial magnetization state, the external magnetic field, the history of loads, and, above all, the chemical composition and non-metallic inclusions [2, 5, 21].

A linear model of a magnetic dipole was developed to study the peripheral excitation method to detect the identification of axial cracks. The model of axial fracture detection in the pipeline was established and the relationship between magnetic flux leakage (MFL) signals and the geometrical characteristics of axial fractures was calculated [14].

An attempt was made to determine the model of ferromagnetic materials in a constant weak magnetic field. The models allow us to reflect the magnetomechanical behavior demonstrated during the experiments performed on the ferromagnetic material depending on the stresses caused by the load in a constant weak magnetic field [12, 16, 18].

There are still several questions and uncertainties concerning the mechanisms of changing the magnetic field intensity occurring in the materials of already functioning

devices, where the exact structure of the material, the number, and size of inclusions and microcracks are unknown [8, 14].

The first attempts were made to monitor changes in the residual magnetic field of structural elements of cranes during their operation, e.g. girders of overhead traveling cranes, to detect places of potential damage before its occurrence [6, 9, 10].

There is still no answer whether the MMM method can be used for online testing of transport devices during their use.

2. Materials and Methods

The research in this article aims to demonstrate the applicability of MMM for the diagnosis of cranes during their operation, using their movement mechanisms.

To determine the level of the influence of the operating parameters of the tested devices on the Hp results during their operation, the level of the intrinsic magnetic field strength of the crane girder was examined depending on:

- load of the crane within its nominal lifting capacity,
- measurement speed,
- the influence of the magnetic field generated by the operation of movement mechanisms powered by electric current.

The flux-gate magnetometer TSC-4M-16 (Tester of Stress Concentration) with scanning device was used for measuring data about stress-induced magnetic flux leakage (MFL) of the crane's girder. The scanning device is manufactured in form of a 4-wheel trolley with flux-gate transducers and a length-counting device (fig. 2). The transducers (magnetometers) installed in the scanning device allows for the measurement of the 2D distribution of SMFL signal along the surface of an inspected structure. The TSC-4M-16 magnetometer allows for the measurement of the magnetic field intensity in the range ±2000 A/m, a basic relative error of 5% for H_p and a sensor accuracy movement of 0.9 mm. The magnetometer TSC-4M-16 is equipped with software for data acquisition and analysis. To reduce measurement errors, 4 measurements were made for each variant of the experiment.

A double-girder overhead travelling crane with a lifting capacity of 1000 kg was selected for the experiment, where the span of the girder was $l = 7.44$ m, wheel spacing of the winch trolley $a = 1$ m (fig. 3), weight of the trolley $m_w = 150$ kg. The girder beams are made of non-alloy steel with the designation S235JR. The transverse dimensions of the girder with the marked surfaces are shown in fig. 4.

Considering the operating characteristics of the tested crane, a test plan was determined to show the changes in the magnetic field strength in the girders under extreme operating conditions. The research plan was marked on both girders. Due to the structure of the girder and the position of the winch trolley, the girder web was determined for testing (figs. 3, 4).

Fig. 2. Tester of Stress Concentration TSC-4M-16 and scanning 4-channel sensor

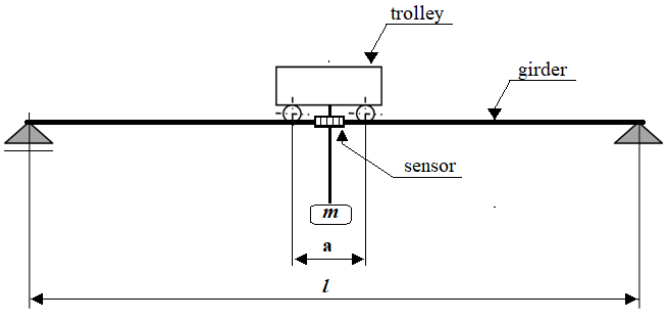

Fig. 3. Diagram of the tested double-girder overhead travelling crane

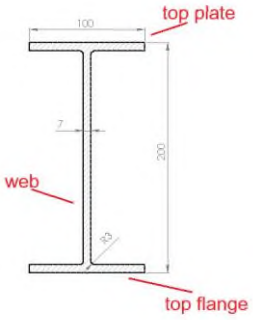

Fig. 4. Cross-section and dimensions of the tested overhead crane girder

3. Results

The winch trolley was placed in the region with the least load on the girders, i.e., on the edge of the bridge. The magnetic field intensity H(x,y) was measured on the prepared device by manually moving the sensor along the tested plane of the spar while the power to the crane was turned off.

During this measurement, the speed of its execution was not determined, the load Q = 0, Vp = undefined. The graph of Hx and Hy waveforms in the spar for the represented sensor is shown in fig. 5.

This test is marked with the symbol A.

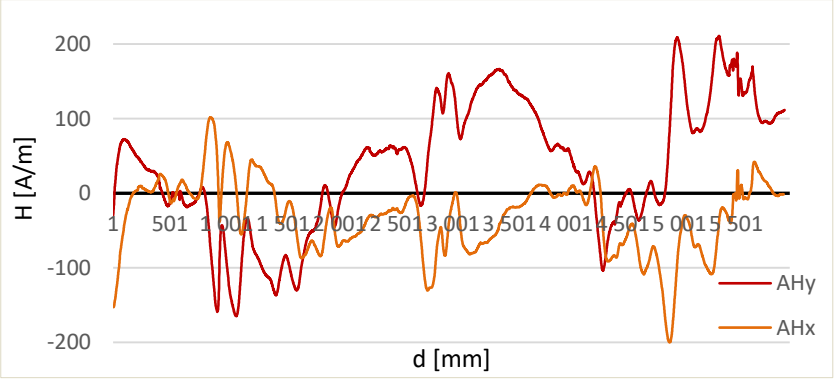

Fig. 5. The course of the magnetic field intensity in the girder - measurement made by hand without the use of crane movement mechanisms for A

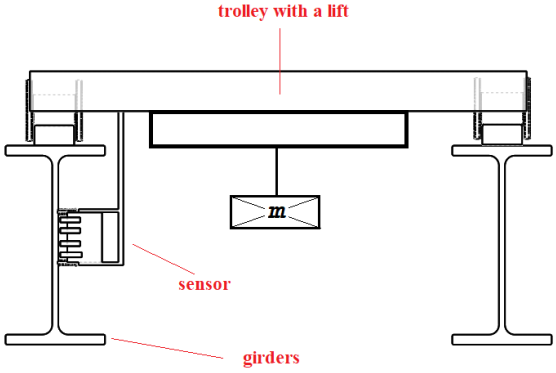

Fig. 6. Position of the magnetometric sensor about the spar and the trolley

A magnetometric sensor was mounted on the trolley with a winch in the middle of its span, on the frame connecting the wheels at an equal distance between the trolley wheels. The magnetometric sensor was mounted in such a way that the magnetometer would scan the spar's designated surface (fig. 6). A trolley with a winch served as a magnetometer shift device. Due to the location of the sensor in the center of the cart, the girder could not be examined over its entire span. The length of the measuring track was limited by the overall dimensions of the trolley and the elements protecting against winch impact and was d = 5792 mm.

The influence of the load H (x, y), the speed of measurements, and the disturbance of the magnetic field generated during the operation of the winch driving mechanism powered by the electric current on the own magnetic field of the designated planes in both girders during the experiments were investigated:

B. after mounting the sensor, the trolley with the sensor was driven through the entire tested span of the spar with a speed of Vp = 4m / min, m_w = 150 kg. We ignore the mass of the sensor with the holder due to its small share in the, to investigate the effect of speed on the results of H (x, y) measurements, the Hp tests of the girders, were repeated at the trolley travel speed Vp = 12m/min, Q = m_w = 150 kg,
C. to investigate the effect of speed on the results of H (x, y) measurements, the Hp tests of the girders were repeated at the trolley travel speed Vp = 12 m/min, Q = m_w = 150 kg,
D. using a winch, the load was lifted with a value of m_o = 1000 kg. The intensity of the residual magnetic field in the girder was measured while the trolley was traveling at a speed of Vp = 4 m/min with a given spar load Q = m_w + m_o = 1150 kg,
E. to check the influence of the measurement speed on the girder loaded with the 1000 kg weight suspended on the winch trolley, a drive was made with a magnetometric sensor at a speed of 12 m/min.

Four measurements were taken for each experiment and the results of the repetitions were analyzed. Due to the repeatability of the results in each replicate of the test variant, only one run for each experiment and only one spar was used for presentation in this publication. Measurement data from four magnetometers were analyzed. Due to a large amount of data, only one of the 4 channels was selected to present the results of the research.

The measurements of the crane loaded with the weight of the trolley and the weight of the lifting capacity made with the use of the trolley as the sensor movement mechanism were analyzed. To clarify the description of the graphs, symbols were used under the experiment carried out:

AHx, AHy - measurement without a load, without the use of a winch trolley,
BHx, BHy - measurement at a speed of Vp = 4 m/min girder loaded only with the weight of the trolley,
CHx, CHy - measurement at a speed of Vp = 12 m/min, the girder loaded only with the weight of the trolley,
DHx, DHy - measurement at a speed of Vp = 4 m/min girder loaded with a trolley weight and a load of 1000 kg,

EHx, EHy – measurement at a speed of Vp = 12 m/min girder loaded with a trolley weight and a load of 1000 kg.

The data from experiments explaining the impact of the speed of the measurement on the girder loaded only with the own weight of the trolley were compared. The results of the measurement of the Hx component are shown in fig. 7, and the Hy component in fig. 8.

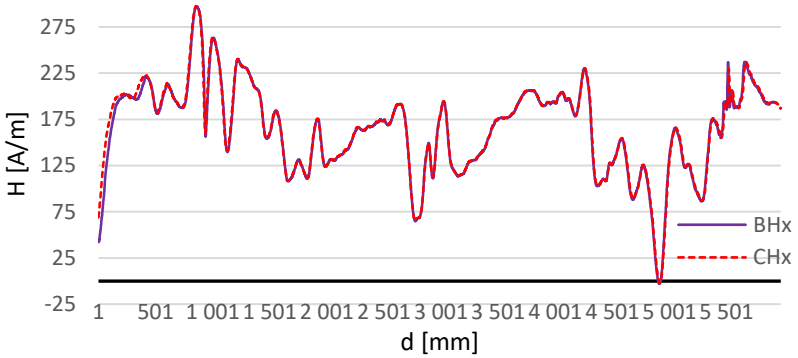

Fig. 7. Hx waveform in the girder for two different measuring speeds 4 m/min and 12 m/min for the girders' load only with the winch's trolley

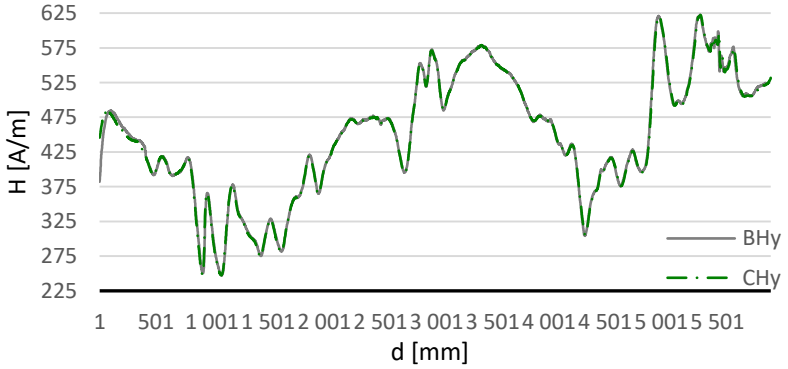

Fig. 8. Hy waveform in the girder for two different measuring speeds 4 m/min and 12 m/min for the girders' load only with the winch's trolley

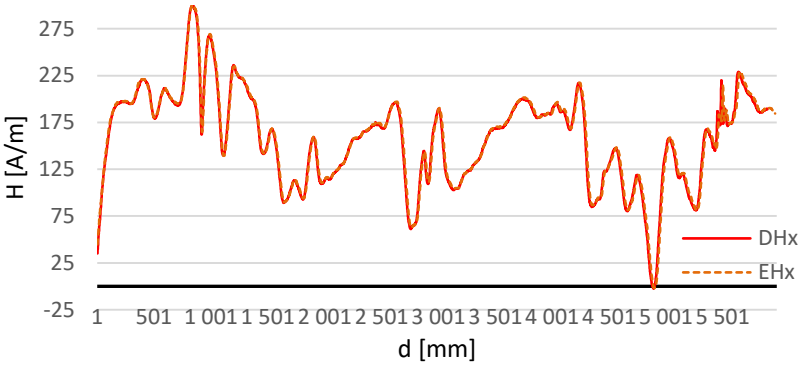

Fig. 9. Hx waveform in the girder for two different measuring speeds 4 m/min and 12 m/min for the load of the girders with a winch trolley and a weight of 1000 kg

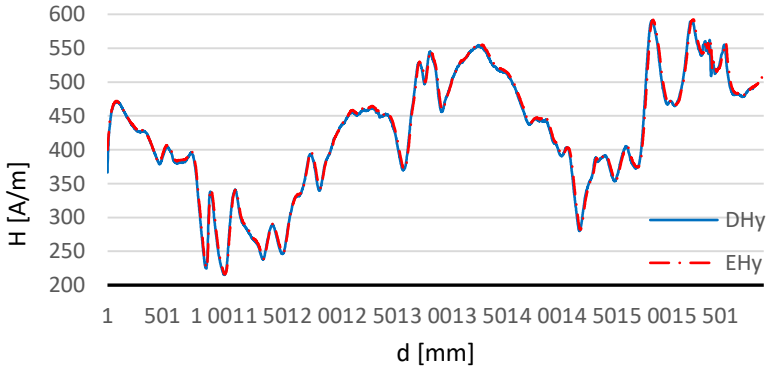

Fig. 10. Hy waveform in the girder for two different measuring speeds 4 m/min and 12 m/min for the load of the girders with a winch trolley and a weight of 1000 kg

The graphs of the measured tangential and normal components obtained at a speed of 4 and 12 m/min, where the measuring system is affected by an additional magnetic field generated by the motor of the trolley movement mechanism, coincide. It can be concluded that the speed of the measurement does not influence the obtained results. The same tests were carried out for girders loaded with an additional 1000 kg mass. The effects are shown in figs. 9 and 10. For a loaded crane, the measurement results also coincide.

To investigate the influence of the load causing the elastic deformation of the crane girders on the size of the own magnetic field, the results of measurements for extreme loads for the same speed Vp = 4 m/min were compared. For the tangential x component (fig. 11) and the normal component y (fig. 12), the measurement results are similar.

They do not completely coincide, slight deviations for Hx can be noticed, while for the Hy component the results for the girder loaded only with the trolley show higher H values by approx. 25 A/m (fig. 12). The same effect is noticeable for a higher measurement speed

at different loads. This effect may be caused by elastic changes that occur in the spar structure. The reason may also be the increased engine power causing a change in the emitted magnetic field. The overhead load is related to the deflection of the girders and the frame of the trolley to which the sensor is attached, it may be related to the displacement of the measuring track about the sensor.

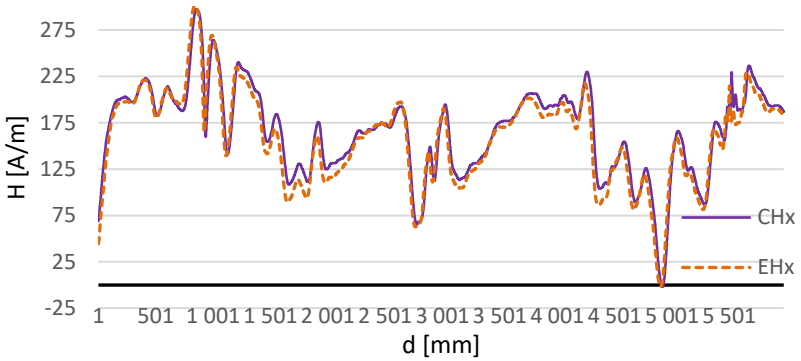

Fig. 11. Hx waveform in the girder for a measurement speed of 4 m/min for extreme loads on the girder

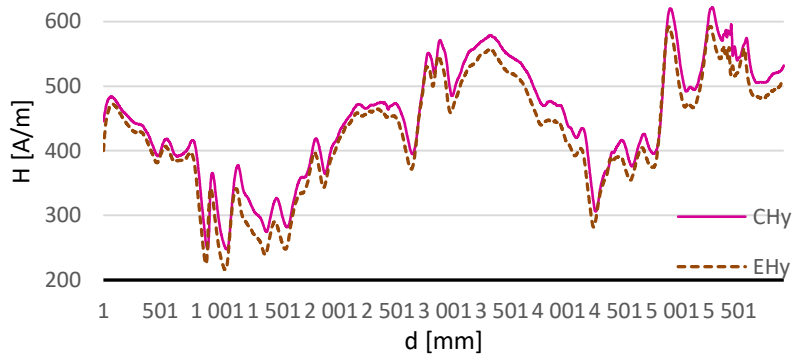

Fig. 12. Hy waveform in the girder for a measurement speed of 4 m/min for extreme loads on the girder

The results obtained during the measurement carried out without the use of the winch's trolley, where there was no influence of the magnetic field from the motion mechanisms, were compared with the measurements made with the use of a trolley with a speed of Vp = 4 m/min at extreme spar loads (figs. 13 and 14). The presented graphs show that the influence of the magnetic field from the winch trolley drives is constant throughout the experiment.

The results obtained during the measurement carried out without the use of the winch's trolley, where there was no influence of the magnetic field from the motion mechanisms, were compared with the measurements made with the use of a trolley with a speed of Vp = 4 m/min at extreme spar loads (figs. 13 and 14). The presented graphs show that the influence of the magnetic field from the winch trolley drives is constant throughout the experiment.

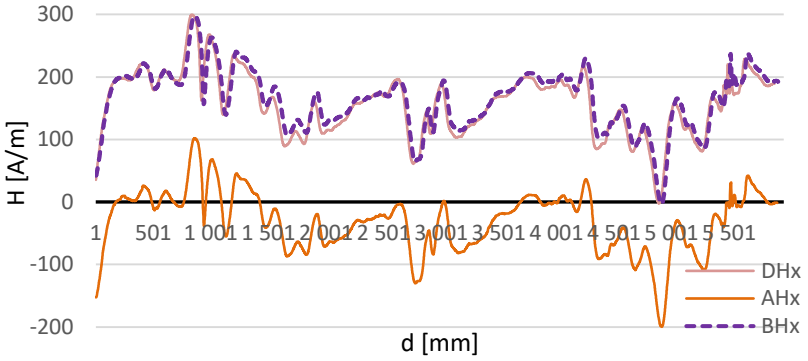

Fig. 13. Comparison of the results of the experiment for the tangent x component

The analyzed Hx and Hy waveforms show a visible influence of the magnetic field generated by the winch trolley motor on the measurement results. Based on the literature and figures 1 and 5, the sites of magnetic anomalies were selected, where Hy = 0, while Hx reaches the local max for experiment A. The points in which the anomaly was demonstrated are presented in tab. 1. For all experiments, the value of H was read at selected points.

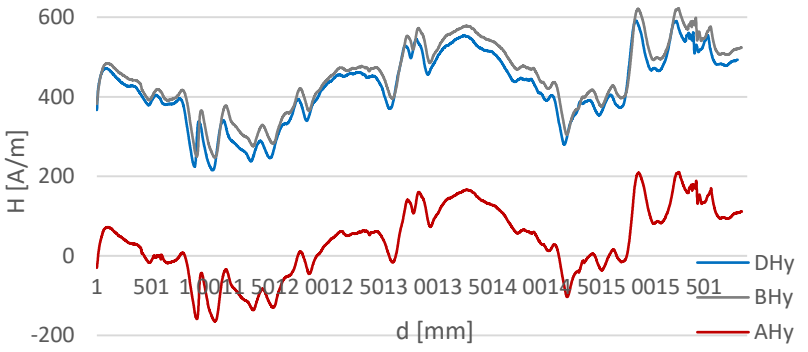

Fig. 14. Comparison of the results of the experiment for the normal y component

Table 1

Hx and Hy values in the magnetic anomaly sites for the conducted experiments

Point	AHy	AHx	BHy	BHx	CHy	CHx	DHy	DHx	EHy	EHx
438	0	24	409	220	408	220	393	217	393	217
1850	0	-78	410	117	411	118	394	121	395	114
2022	0	-65	412	130	411	130	394	115	395	116
2692	0	-21	407	173	407	173	370	146	375	158
2748	0	-104	412	90	412	89	417	65	408	71
4250	0	34	405	228	408	226	340	215	353	217
4531	0	-61	413	134	411	134	391	140	391	137
4581	0	-41	410	154	411	154	370	142	377	147
4721	0	-98	418	99	415	98	405	103	403	97
4783	0	-72	410	125	412	126	379	106	384	112
4873	0	-159	412	37	408	43	418	8	404	19

Graphical presentation of tabular data for each point of the determined magnetic anomalies in the tested spar is shown in the graphs shown in fig. 15.

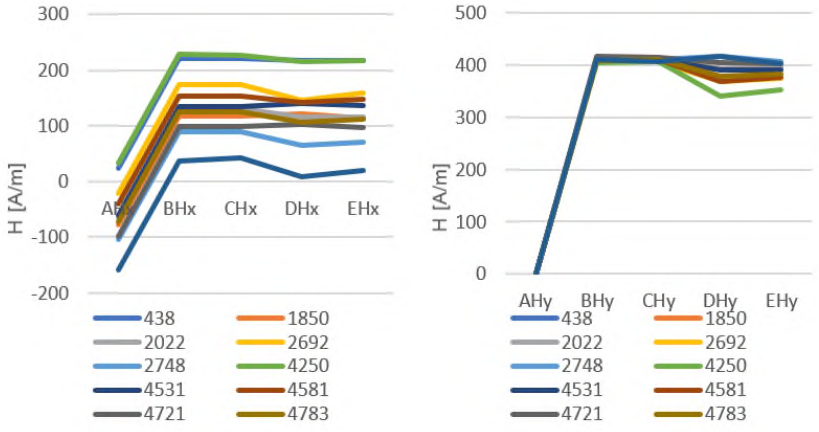

Fig. 15. H-value at designated points for the performed experiments

The results of experiment A differ significantly from the others. There is a noticeable change in the magnetic field during Hp measurements with the use of a winch trolley. The results obtained with the use of the winch trolley, differing in speed and weight of the tested spar load, are linear, which proves the lack of influence of these parameters on the intensity of the magnetic field. Based on the graphs in fig. 15 and the calculations of the increase in

ΔH presented in tab. 2, a smaller increase can be noticed for the experiments using the maximum load of the crane. For the designated measuring section of 4250-4850 mm, there is a welded joint on the spar beam on the entire cross-section of the profile. The chemical composition of the weld differs from that of the spar material, which affects the behavior of the magnetic field at this point. In a welded joint, there may be stress due to welding treatment and elastic deformation after loading the beam. Comparisons with magnetic field tools after using tool-less measurement tools.

Table 2

Hx and Hy changes depending on the load and measurement speed

Point	BHy-AHy	CHy-AHy	DHy-AHy	EHy-AHy	BHx-AHx	CHx-AHx	DHx-AHx	EHx-AHx
438	409	408	393	393	196	197	194	194
1850	410	411	394	395	195	196	199	192
2022	412	411	394	395	196	196	181	182
2692	407	407	370	375	194	194	167	179
2748	412	412	417	408	194	194	170	175
4250	405	408	340	353	195	192	181	183
4531	413	411	391	391	196	195	202	198
4581	410	411	370	377	195	195	184	188
4721	418	415	405	403	197	197	202	195
4783	410	412	379	384	197	198	179	184
4873	412	408	418	404	196	202	167	178
Av.	411	410	388	389	195	196	184	186

The results show the growth tab. 2. For the measurements without changes with the measurement of the first A, it is approx. ΔH =410.5 A/m for the y component, and ΔH=195.5 A/m for the x component. After the crane is loaded with a mass of 1000 kg, this increase is smaller and amounts to ΔH =388.5 A/m for the y component and ΔH =185 A/m for the x component.

The level of the magnetic field strength was measured near the trolley of the winch, at a distance allowing the measurement without the influence of the spar's magnetic field. With the device turned off, Hx = -6 A/m, Hy = 158 A/m, and when the trolley's driving mechanism is turned on, it reaches the value of Hx = 186 A/m Hy = 562 A/m.

Figure 15 shows the magnitude of the changes occurring during the different variants of the measurements performed. The most stable method of Hp measurements for girders is the method using a winch cart with load m_o =0kg. For the selected points it does not show any differences when changing the measurement speed. After determining the disturbances

of the magnetic field strength caused by the action of the winch cart, these measurements can be considered to reflect the actual state of magnetization of the tested girders.

As is shown in fig. 16, the value of H is affected by the magnetic field generated by powering the trolley's driving mechanism with an added bias of 192 A/m and 404 A/m for the tangential and normal components respectively. Measurements for the loaded mechanism were not performed in fig. 16. Before carrying out measurements using the MMM method, it is necessary to measure the intensity generated during the operation of the device that will serve as a drive for the magnetometric sensor to determine the excess disturbing the actual measurement. To obtain a measurement result that is not affected by magnetic field interference from the crane drive equipment, the values measured for the trolley must be subtracted from the values of the girder magnetic field strength measured with the winch trolley activated.

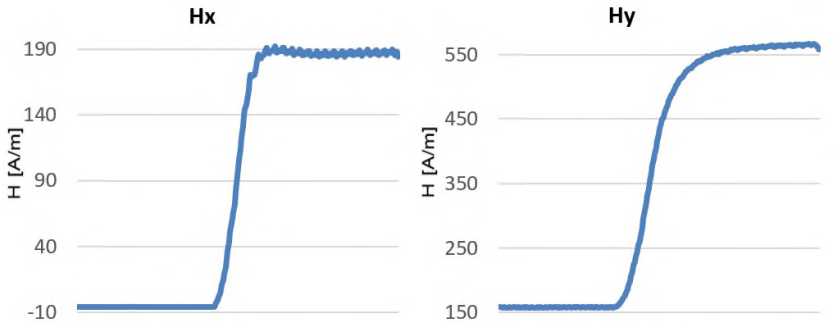

Fig. 16. Dependence of Hx and Hy values on the work of the winch's trolley

4. Conclusions

The presented work describes the use of the metal magnetic memory method for cranes diagnostics. The structure is exposed to high stresses related to the transferred load, which is associated with plastic deformations resulting from material fatigue.

Measurement tests were performed on a device located in a research laboratory. During the measurements, it was ensured that there was no influence of the additional magnetic field from other devices not included in the crane.

Diagnostic tests of crane girders using non-destructive methods require measurements at considerable heights and sections, which makes it difficult to perform them quickly and accurately. The safest and the most convenient way is to fix the measuring devices on the crane trolley in a way that allows scanning the appropriate plane of the girder. Thanks to the drive of the trolley movement mechanism, it is possible to measure with the same set speed safely and accurately without the effect of changing the direction and the direction of the measurement axis. The results show that the speed of measurement has no significance

and does not affect the results in any way. However, one should consider the magnetic field interference from the trolleys and winch driving devices. Research has shown that these disturbances are permanent while driving.

The disturbance parameter is easy to calculate, knowing the course Hp of the determined measuring section of the tested spar and the results of measurement Hp of the same section made with the use of the winch trolley.

The increase in the value of the magnetic field strength ΔH for the x and y components between the first measurement of the determining section and the measurement made with the use of the winch trolley travel mechanism is the determinant of the allowance by which the measurement results should be corrected to obtain the correct magnetic field strength data in the entire spar. It is also possible to determine the size of disturbances by measuring the magnetic field strength at an appropriate distance from the tested surface and the disturbing device during its rest and operation. Performing tests at extreme loads have proved that the load has a slight influence on the measurement results, approx. 5%. The conducted research indicates the possibility of using the metal magnetic memory method to facilitate the diagnosis of crane girders. Using the trolley of the crane's winch as a drive for the magnetometric sensor can automate and improve the girder diagnostics using the metal magnetic memory method. The use of a winch carriage for Hp measurements greatly improves the test flow, the measurement is made at uniform speed on a constant trajectory without forcibly detaching the magnetometer from the girders to move it.

Early detection of potential crane damaged areas, and their observation will allow a quick response about repair or taking the equipment out of service to ensure safe use of the crane.

To correctly assess the thesis put forward in this article, it will be necessary to perform measurements on cranes in industrial conditions with a diversified history of loads and drive devices winches.

Acknowledgement
The work has been financially supported by the Polish Ministry of Education and Science.

5. References

1. Bao S., Fu M., Hu S., Gu Y., Huangjie L.: A review of the metal magnetic memory technique. ASME 2016 35th Busan, South Korea 2016.
2. Bao S., Lou H., Zhao Z.: Evaluation of stress concentration degree of ferromagnetic steels based on residual magnetic field measurements. J Civ Struct Heal Monit. 2020.
3. Dubov A.A.: Detection of Metallurgical and Production Defects in Engineering Components Using Metal Magnetic Memory. Metallurgist, 2015.
4. Dubov A., Kolokolnikov S.: Assessment of the material state of oil and gas pipelines based on the metal magnetic memory method. Weld World, 2012.

5. Huang H., Yao J., Li Z., Liu Z.: Residual magnetic field variation induced by applied magnetic field and cyclic tensile stress. NDT E Int. 2014.
6. Juraszek J.: Residual magnetic field non-destructive testing of gantry cranes. Materials. 2019.
7. Kolokolnikov S.M., Dubov A.A., Marchenkov A.Y.: Determination of mechanical properties of metal of welded joints by strength parameters in the stress concentration zones detected by the metal magnetic memory method. Weld World, 2014.
8. Kosoń A., Szpytko J.: Investigation of the Impact of Loadon the Magnetic Field Strength of the Crane by the Magnetic Metal Memory Technique. Materials, 2020.
9. Kosoń-Schab A., Szpytko J.: Magnetic metal memory in the assessment of the technical condition of crane girders for the needs of safety. Journal of Konbin, Vol. 49, Iss. 4, 2020, DOI 10.2478/jok-2019-0075.
10. Kosoń-Schab A., Smoczek J., Szpytko J.: Magnetic Memory Inspection of an Overhead Crane Girder – Experimental Verification. Journal of KONES, 2019.
11. Li Z., Dixon S., Cawley P., Jarvis R., Nagy P.B.: Study of metal magnetic memory (MMM) technique using permanently installed magnetic sensor arrays. AIP Conf Proc., 2017.
12. Li J., Xu M., Leng J., Xu M.: Modeling plastic deformation effect on magnetization in ferromagnetic materials. J Appl Phys, 2012.
13. Liu B., He L-y., Zhang H., Cao Y., Fernandes H.: The axial crack testing model for long distance oil-gas pipeline based on magnetic flux leakage internal inspection method, Measurement, 2017, DOI: 10.1016/j.measurement.2017.02.051.
14. Roskosz M., Bieniek M.: Evaluation of residual stress in ferromagnetic steels based on residual magnetic field measurements. NDT E Int, 2012.
15. Roskosz M., Gawrilenko P.: Analysis of changes in the residual magnetic field in loaded notched samples. NDT E Int, 2008.
16. Shi P.: Magneto-mechanical model of ferromagnetic material under a constant weak magnetic field via analytical anhysteresis solution. J Appl Phys, 2020.
17. Shi P., Su S., Chen Z.: Overview of Researches on the Nondestructive Testing Method of Metal Magnetic Memory: Status and Challenges. J Nondestruct Eval, 2020.
18. Wang Z.D., Deng B., Yao K.: Physical model of plastic deformation on magnetization in ferromagnetic materials. J Appl Phys, 2011.
19. Vlasov V.T., Dubov A.A.: Physical Bases of the Metal Magnetic Memory Method. ZAO "TISSO", Moscow 2004.
20. Villegas-Saucillo J., Díaz-Carmona J.J., Cerón-Álvarez C.A., et al.: Measurement system of metal magnetic memory method signals around rectangular defects of a ferromagnetic pipe. Appl Sci, 2019.
21. Zhang K., Zhang J., Jin W., Mao J., Xu Y., Li Q.: Characterization of fatigue crack propagation of pitting-corroded rebars using weak magnetic signals. Eng Fract Mech, 2021.